Development of a Whole-Sensitive Teleoperated Robot Arm using Torque Sensing Technique

Dzmitry Tsetserukou[*] Riichiro Tadakuma[*] Hiroyuki Kajimoto[*†] Naoki Kawakami[*]
Susumu Tachi[*]
(*) The University of Tokyo, Department of Information Physics and Computing, Japan
(†) The University of Electro-Communications, Japan*
E-mail: dima_teterukov@ipc.i.u-tokyo.ac.jp, r-tadakuma@aist.go.jp, kajimoto@hc.uec.ac.jp, kawakami@ star.t.u-tokyo.ac.jp, tachi@ star.t.u-tokyo.ac.jp

Abstract

In this paper, we concentrate on the design of a new whole-sensitive robot arm enabling torque measurement in each joint by means of developed optical torque sensors. When the contact of arm with an object occurs, local impedance algorithm provides active compliance of corresponding robot arm joint. Thus, the whole structure of the manipulator can safely interact with unstructured environment. The detailed design procedure of the 4-DOF robot arm and optical torque sensors is described in the paper. The gravity compensation algorithm was elaborated and verified by implementation of the local impedance control of a simple two-link arm manipulator.

1. Introduction

In the recent years, robots that are able to perform work in human daily environments, such as offices, hospitals and homes, has been successfully developed [1]. This causes the necessity to support assurance of safe human-robot-environment interaction.

In teleoperation systems, the same problem arises since a slave robot controlled by the human operator mainly performs the manipulations in unknown and unstructured environment. Moreover, teleoperated robot interacts with human in various cooperative tasks. In these applications, the force sensing ability is a crucial aspect of safe interaction in the environment. The NASA/DAPRA Robonaut teleoperated robot has a new tactile glove instrumented with 19 force sensors to grasp control realization [2]. The operator moves the robot arm until the palm contacts the object. However, the rest part of the robot arm still carries dangerousness for the surrounding objects.

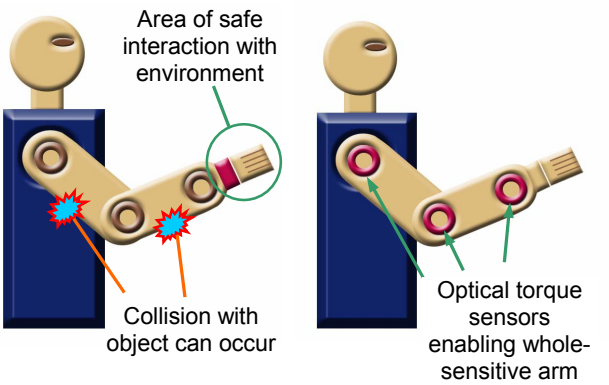

Figure 1. Concept of whole-sensitive robot arm realization

The whole-sensitive arm manipulator covered with a sensitive skin capable of detecting nearby objects was designed by V. J. Lumelsky et al. [3] to avoid collisions in time-varying environment. The sensitive skin is able to identify the point of collision rather than the external force value. S. Morinaga and K. Kosuge [4] proposed collision detection system without using external sensors. The system recognizes collisions based on the difference between the actual input torque applied to the joints and the reference input torque calculated from manipulator dynamics. However, inaccuracy of the dynamic model parameters deteriorates sensitivity threshold up to 17.4 N at the elbow joint. The dexterous robot-human cooperative work requires continuous measurement of force in range of 0-50 N.

We have successfully developed master-slave robot systems (TELESAR I and TELESAR II) based on the

Second Joint EuroHaptics Conference and Symposium on Haptic Interfaces for Virtual Environment and Teleoperator Systems (WHC'07)
0-7695-2738-8/07 $20.00

telexistence concept [5]. The safe working area is provided only around the wrist where the force sensor is attached (Fig. 1a).

To realize friendly human-robot interaction, our primary idea is devoted to the design of whole-sensitive slave robot arm (by using distributed torque sensors in each joint) and compliant motion realization when contact occurs (Fig. 1b). The main issue here is the cost of the commercially available compact force/torque sensors providing redundant information for the case of only one-axis moment measurement. Besides, to incorporate the sensors with unique robot design, the additional mounting plates have to be installed, making the joint structure bulky. The authors [6] implemented strain-gauge-based torque sensors to facilitate torque-controlled lightweight robot. However, strain gauges have such inherent drawbacks as considerable electrical noise level, easy breakableness, complicated calibration procedure, etc. Work experience with strain-gauge-based 6-axis force/torque sensor showed inevitability of implementation of the additional digital low-pass filter to get readable data scarifying bandwidth of signal as small as 60 Hz.

In order to realize impedance control of each arm joint, we developed new optical torque sensors having high reliability, good accuracy, easy mounting procedure, and low price. The 4-DOF anthropomorphic robot arm with torque measuring ability in each joint has been designed for the slave robot. To extract the value of contact force from the torque sensor signal, we propose the procedure of gravity force estimation.

2. Design of whole-sensitive anthropomorphic robot arm

In order to remove mechanical subsystems without disassembling the main structure when the failures do occur, we were using a modular approach while designing anthropomorphic robot arm. Therefore, we selected CSF-series gear head type of Harmonic Drive instead of compact and lightweight component type. The Harmonic drive offers such advantages as accurate positioning, high torque capability, torsional stiffness, and high single stage ratios. Most of the robot parts were made from aluminium alloys to obtain as much lightweight structure as possible. The distribution of the arm joints replicates the human arm structure in order to make it easy to operate using kinesthetic sensation during teleoperation. Developed teleoperated robot arm has 4-DOF. Each joint is equipped with optical torque sensor. The sizes and appearance of the arm were decided so that the sense of incongruity during interaction with human is avoided. We kept the arm proportions the same as in average height human: upper arm length L_1 - 0.308 m; upper arm circumference - 0.251 m (diameter 0.080 m); forearm length L_2 - 0.241 m; forearm circumference - 0.189 m (diameter 0.06 m). The 3D CAD model of developed arm and coordinate systems based on Denavit-Hartenberg convention are represented in Fig. 2.

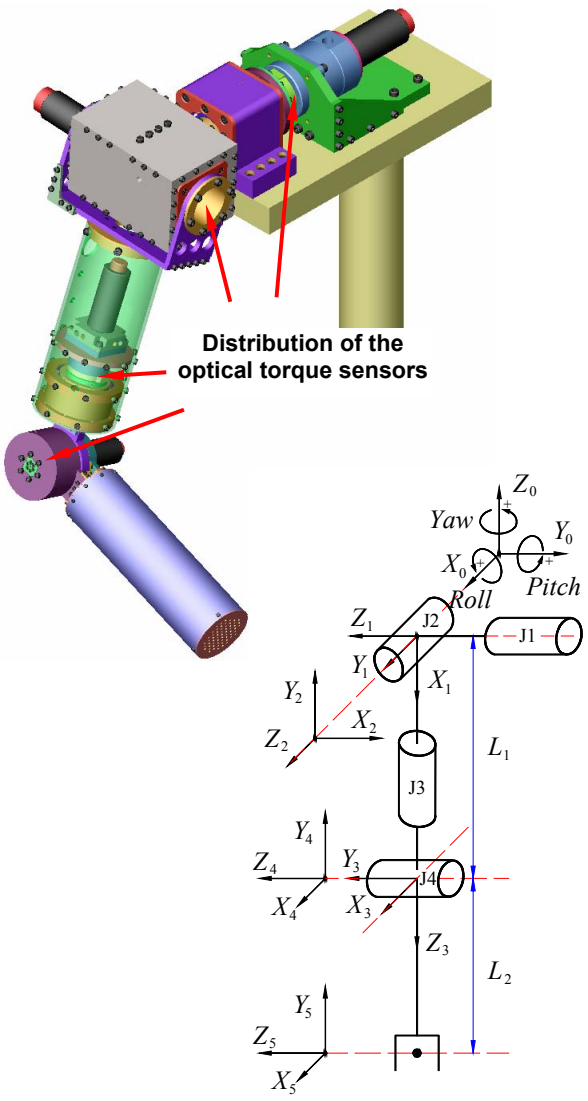

Figure 2. 3D CAD arm model and coordinate systems

The principal specifications and kinematic parameters of the developed arm are listed in Table 1 and Table 2, respectively.

0-7695-2738-8/07 $20.00

Table 1. Principal specifications

Parameters		New slave arm
Mobility range (Human arm), [deg]	Shoulder: J1, Pitch	-180 to 180 (-60 to 180)
	Shoulder: J2, Roll	-180 to10 (-165 to 0)
	Shoulder: J3, Yaw	-180 to 180 (-60 to 180)
	Elbow: J4, Pitch	0 to 112 (0 to 130)
Motor power, [W]	Shoulder: J1, Pitch	90, Maxon RE 35
	Shoulder: J2, Roll	60, Maxon RE 35
	Shoulder: J3, Yaw	26.6, Faulhaber 2657
	Elbow: J4, Pitch	26.6, Faulhaber 2657
Drive rated torque [Nm], (type)	Shoulder: J1,Pitch	7.8, (CSF-14-GH)
	Shoulder : J2,Roll	7.8, (CSF-11-2XH)
	Shoulder: J1, Yaw	5, (CSF-11-2XH)
	Elbow: J4, Pitch	5, (CSF-11-2XH)

Table 2. Denavit-Hartenberg parameters of the robot arm

i	α_{i-1} [deg]	a_{i-1} [m]	d_i [m]	θ_i [deg]
1	90	0	0	θ_1 - 90
2	-90	0	0	θ_2 + 90
3	90	0	L_1	θ_3 + 90
4	-90	0	0	θ_4 - 90
5	0	L_2	0	0

The motors are equipped with encoders having 512 pulses per revolution. To prevent influence of bending moment on the torque value measurement, the simple supported loaded shaft configuration was realized.

In addition to contact force, torque sensor continuously measures the gravity and dynamic load. Teleoperated slave robot arm usually works with small speeds; and dynamics influence is negligible comparing with gravity load. Besides, it cannot be accurately calculated. To extract the value of contact force from a sensor signal, we elaborated algorithm for calculation of torque caused by contact with an object.

3. New optical torque sensor design

Optical approach to torque measurement considers measuring displacement between unmovable and flexible parts of the torque sensor by means of light source and photosensor. Comparing to electrical and electromagnetic methods, it ensures better noise immunity, easier sensing element installation procedure, high robustness, and low cost manufacturing. S. Hirose and K. Yoneda [7] proposed to use a split type photodiode to detect the displacement of the light source (LED) caused by force applied in two directions. In cooperation with Minebea Co. OPFT series of the 6-axes optical force sensors were manufactured [8]. These transducers are compact, lightweight, and low in cost. However, they suffer from complicated calibration procedure, require application of Digital signal processor for real-time computation of measured force, and have an average accuracy of 5% of Full Scale.

Our objective was to develop a torque sensor for the specific application – teleoperated robot arm. While elaboration of the optical torque sensor structure, we followed the guidelines listed below:

1. Addition of the torque sensor to a robot joint should cause a minimal modification in kinematics and dynamics. Therefore, lightweight sensor with small width is preferable.
2. High Signal-to-noise ratio to ensure high resolution of torque measurement.
3. To avoid mechanical resonance, torsional stiffness of the sensor should not considerably reduce the natural frequency of the robot arm.
4. Mechanical structure should be machined from a single piece of metal in order to eliminate hysteresis.
5. Reliable, simple to manufacture, and low in cost.

The distinctive feature of our method is application of the ultra-small size photointerrupter (PI) RPI-121 as a sensitive element to measure relative motion of the sensor components. The linear section of the transferring characteristic of PI can be used for detection of the relative displacement of an object [9]. Compact overall dimensions of the sensor can be realized due to the small dimensions of PI (RPI-121: 3.6 mm × 2.6 mm × 3.3 mm) and its weight (0.05 g). Furthermore, PI also has negligible influence from the electromagnetic field and stray light. We developed several sensor prototypes to find out the optimal solution [10]. The optical torque sensor is set between the harmonic drive and driven shaft of the joint (Fig.3).

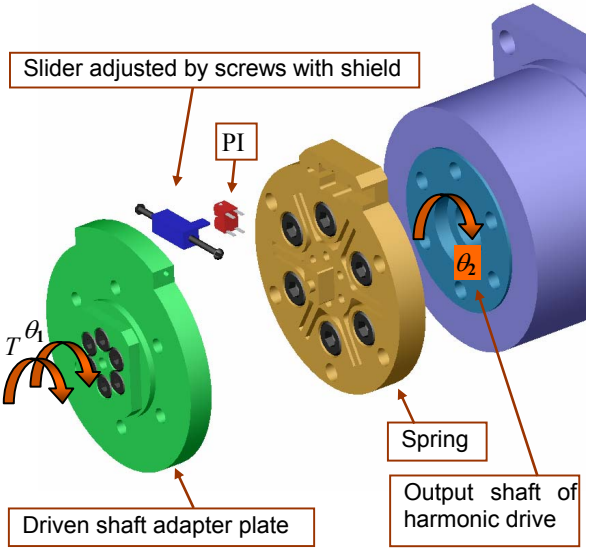

Figure 3. Structure of the optical torque sensor

0-7695-2738-8/07 $20.00

When a load is applied to the arm, the spring in corresponding joints is deflected. This causes the adapter plate rotation with small angle of twist, θ. The shield displacement is detected by the degree of interruption of infrared light that falls on the phototransistor. Thus, the magnitude of output signal of the PI corresponds to the applied torque. The relationship between the sensed torque, T, and the angle of twist is the following:

$$T = k\theta = k\left(\theta_1 - \theta_2\right) = k\,\Delta x / R\,, \qquad (1)$$

where k – torsional stiffness of the spring member, Δx – displacement of the shield in tangential direction, R – distance from the sensor center to the middle axis of the shield plate in radial direction. The drawing of the hub-spoke-shaped spring is presented in Fig. 4.

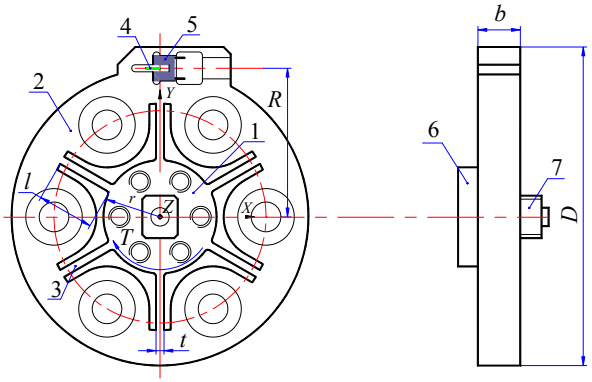

Figure 4. Hub-spoke structure layout

The detector consists of the inner part 1 connected by the flexure 3 with the outer part 2, fixed PI 5, and shield plate 4. For axial alignment of the spring with output shaft of the harmonic drive, we provided for the round shape protrusion 6. The protrusion 7 is intended for increasing the transferring torque rate. The torsional stiffness of the sensor [11] is derived from:

$$k = 4NEI\left(\frac{1}{l} + \frac{3r}{l^2} + \frac{3r^2}{l^3}\right), \qquad (2)$$

where N – number of spokes, E – modulus of elasticity, I – moment of inertia of the spoke cross section, l – the spoke length, and r – inner radius of the sensor.

The value of I can be calculated as follows:

$$I = bt^3/12\,, \qquad (3)$$

where b – beam width, t – beam thickness.

The sensing range of the sensors was decided based on the value of torque in each joint caused by gravity force and contact force of ± 25 N at the tip of the arm. Such materials as high yield-strength stainless steel 17-4PH, 13-8 VAR as well as AISI 4135 and 4130 steel can be employed for manufacturing the spring member. We decided to use AISI 4135 steel with tensile yield strength σ_{yield} of 785 MPa. The results of analysis using FEM demonstrate tangential displacement in mm (Fig. 5a) and von Mises stress in MPa (Fig. 5b) of the loaded springs in elbow joint J4 under the torque T_Z of 4.5 Nm.

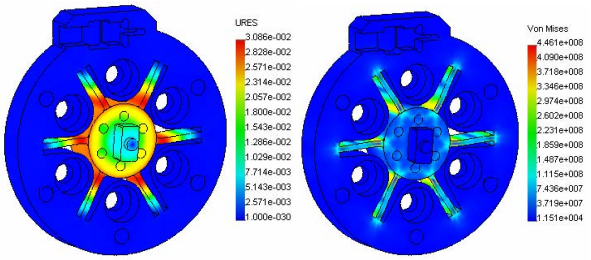

a) Tangential displacement b) von Mises stress

Figure 5. Results of analysis using FEM

The torsional stiffness is calculated from Eq. (1) using tangential displacement value (Fig. 5a). The sensor was manufactured from one piece of steel using wire electrical discharge machining (EDM) cutting. Components and assembly of the torque sensor incorporated in third/forth joints are presented in Fig. 6.

Figure 6. Torque sensor of elbow joint

The test rig for calibration of the optical sensor has been developed (Fig.7). Loading torque was created by means of attachment of reference weights to the lever arm.

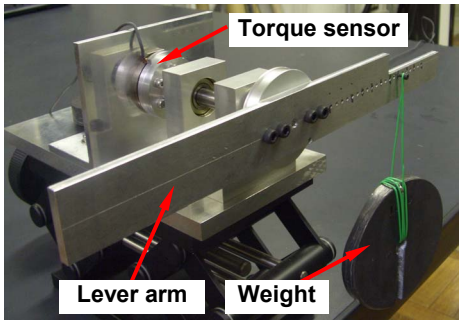

Figure 7. Calibration setup

0-7695-2738-8/07 $20.00

The calibration was realized by changing the mass of attached weights as well as lever length, and measuring the output signal from the PI. Calibration results are presented in Fig. 8.

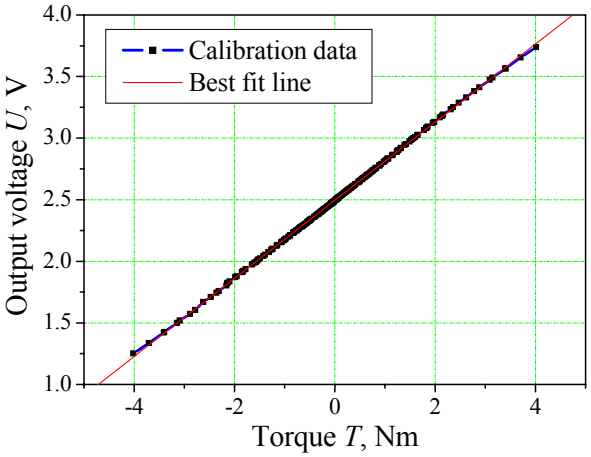

Figure 8. Output vs. loading torque

In order to determine sensitivity and non-linearity of the optical torque sensor, we used the best fit line approach. Calculated sensitivity of the transducer attached to the joint J4 equals 0.317 V/Nm. Non-linearity of 2.5 % of Full Scale was calculated using maximum deviated value from the best fit line. Specifications of the developed optical torque sensors and analogous 6-axis T/F sensor are listed in Table 3.

Table 3. Technical specifications

Sensor	First joint	Second joint	Third/ fourth joint	ATI Mini 45 SI-290-10 [12]
Sensing range, [± Nm]	12.5	10.5	4.5	10.0
Torsional stiffness, [Nm/rad]	3 230	2 730	950	35 000
Factor of safety	1.76	1.7	1.82	5.4
Outer diameter [mm]	45	42	37	45
Thickness, [mm]	7.0	6.0	5.0	15.7
Mass, [g]	68.4	49.8	34.2	92.0

The main advantages of the ATI sensors [12] are high torsional stiffness and large factor of safety. Nevertheless, such features as compactness, easy manufacturing process, low cost, and simple calibration procedure make the developed sensors preferable for torque measurement in robot arm joints.

4. Gravity compensation algorithm and impedance control implementation

In this section, we consider the problem of computing the joint torques corresponding to the gravity forces acting on links with knowledge of kinematics and mass distribution. It is assumed that, due to small operation speed, the angular accelerations equal zero. The Newton-Euler dynamics formulation was adopted. In order to simplify the calculation procedure, the effect of gravity loading is included by setting linear acceleration of reference frame ${}^{0}\dot{\vartheta}_{0} = G$, where G is the gravity vector. First, link linear accelerations ${}^{i+1}\dot{\vartheta}_{C_{i+1}}$ of the center of mass (COM) of each link are iteratively computed for $i = 0$ to $i = 4$ (4). Then, gravitational forces ${}^{i+1}F_{i+1}$ (5) acting at the COM of the first and second link ($i = 2$ and $i = 4$) are computed:

$$ {}^{0}\dot{\vartheta}_{0} = g\hat{Z}_{0};\ {}^{i+1}\dot{\vartheta}_{C_{i+1}} = {}^{i+1}R_{i}\,{}^{i}\dot{\vartheta}_{i} \quad (4) $$

$$ {}^{i+1}F_{i+1} = m_{i+1}\,{}^{i+1}\dot{\vartheta}_{C_{i+1}}, \quad (5) $$

where m_{i+1} – mass of the link $i+1$, ${}^{i+1}R_{i}$ – matrix of rotation between successive links calculated using Denavit-Hartenberg notation (Table 2).

While inward iterations, we calculate force ${}^{i}f_{i}$ (6) and torques ${}^{i}n_{i}$ (7) acting in the coordinate system of each joint. In the static case, the joint torques caused by gravity forces are derived by taking Z component of the torque applied to the link (8).

$$ {}^{i}f_{i} = {}^{i}_{i+1}R\,{}^{i+1}f_{i+1} + {}^{i}F_{i} \quad (6) $$

$$ {}^{i}n_{i} = {}^{i}_{i+1}R\,{}^{i+1}n_{i+1} + {}^{i}P_{C_i} \times {}^{i}F_{i} + {}^{i}P_{i+1} \times {}^{i}_{i+1}R\,{}^{i+1}f_{i+1} \quad (7) $$

$$ \tau_{i} = {}^{i}n_{i}^{T}\,{}^{i}\hat{Z}_{i}, \quad (8) $$

where ${}^{i}P_{C_i}$ – vector locating the COM for the link i, ${}^{i}P_{i+1}$ – vector locating the origin of the coordinate system $i+1$ in the coordinate system i.

The joint torques were calculated using the approach cited above. The experiment with simple 2-link arm (Fig. 9a) was conducted in order to measure the joint torque caused by gravity forces and estimate the measured error by comparison with reference model. The system consists of: DC motors with speed reducers (gear ratios of 2548) to guarantee very low backdriving of joints; manufactured torque sensors (sensing range is ±0.8 Nm); and rigid links. The plot of measured (while rotating) and calculated values of torque acting on the first joint is shown in Fig. 9b.

0-7695-2738-8/07 $20.00

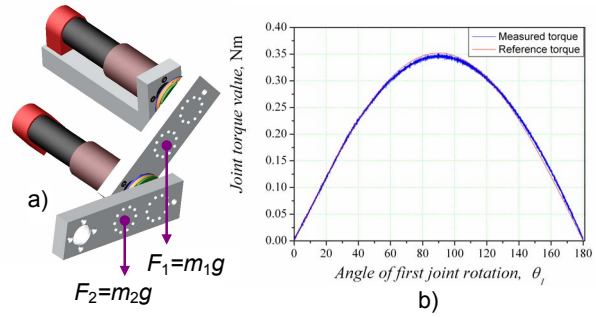

Figure 9. Experimental setup and measurement results

The error of the torque value measurement was considered as a threshold magnitude when contact occurs.

The local impedance control was realized for 2-link arm to ensure safety in interaction using gravity compensation approach. Results of response are shown in Fig. 10. We used the following equation describing desired dynamics of robot joint *i* in joint space:

$$\tau_{EXTi} = J_{di}\Delta\ddot{\theta}_i + D_{di}\Delta\dot{\theta}_i + K_{di}\Delta\theta_i;\ \Delta\theta_i = \theta_{ci} - \theta_{di}, \quad (9)$$

where τ_{EXTi} – torque applied to joint *i* and caused by external and gravity forces, J_{di} – desired inertia, D_{di} – desired damping, K_{di} – desired stiffness, θ_{ci} – output joint angle of the impedance model, θ_{di} – desired joint angle.

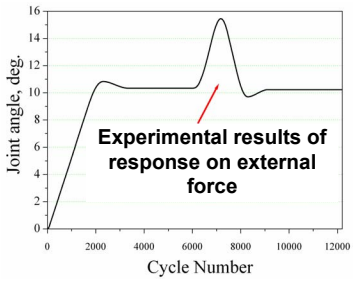

Figure 10. Response graph

5. Future work

The developed robot arm has been already assembled. In near future, we will start to make experiments. Implementation of described approach can significantly contribute to safety improvement of human-robot interaction. Proposed torque sensor eventually diminishes stiffness of the arm and introduces angular error. However, it does not deteriorate the performance of human-robot interaction. The robot arm with torque sensing ability can also be applied as a haptic device. The user can manipulate it in impedance control mode to perform action with remote objects.

6. References

[1] K. Kaneko, F. Kanehiro, S. Kajita, et al. "Humanoid Robot HRP 2", *Proc. of the 2004 IEEE Int. Conf. on Robotics and Automation*, New Orleans, 2004, pp. 1083-1090.

[2] M.A. Diftler, C. J. Culbert, R. O. Ambrose, Jr. R. Platt, and W. J. Bluethmann, "Evolution of the NASA/DARPA Robonaut Control System", *Proc. of the 2003 IEEE Int. Conf. on Robotics and Automation*, Taipei, 2003, pp. 2543-2548.

[3] V. J. Lumelsky and E. Cheung, "Real-time Collision Avoidance in Teleoperated Whole-sensitive Robot Arm Manipulators", *IEEE Trans. on Systems, Man, and Cybernetics,* vol. 23, no. 1, 1993, pp.194-203.

[4] S. Morinaga, and K. Kosuge, "Compliant Motion Control of Manipulator`s Redundant DOF based on Model-based Collision Detection System", *Proc. of the 2004 IEEE Int. Conf. on Robotics and Automation*, New Orleans, 2004, pp. 5212-5217.

[5] R. Tadakuma, Y. Asahara, H. Kajimoto, N. Kawakami, and S. Tachi, "Development of Anthropomorphic Multi-D.O.F. Master-slave Arm for Mutual Telexistence", *IEEE Trans. on Visualization and Computer Graphics*, vol. 11, no. 6, November 2005, pp. 626-636.

[6] G. Hirzinger, A. Albu-Schaffer, m. Hahnle, I. Schaefer, and N. Sporer, "On a New Generation of Torque Controlled Light-Weight Robots", *Proc. of the 2006 IEEE Int. Conf. on Robotics and Automation*, Seoul, 2004, pp. 3356-3363.

[7] S. Hirose and K. Yoneda, "Robotic Sensors with Photodetecting Technology", *Proc. of 20th Int. Symp. on Industrial Robotics*, 1989, pp. 271-278.

[8] A. Kitamura, S. Adachi, and S. Tanabe, "Optical Displacement Sensor and External Force Detecting Device", U. S. Patent 7 057 154 B2, Jun 6, 2006.

[9] "*Photointerrupter Design Guide*". Product catalog of ROHM, pp. 6-7, 2005.

[10] D. Tsetserukou, R. Tadakuma, H. Kajimoto, and S. Tachi, "Optical Torque Sensors for Implementation of Local Impedance Control of the Arm of Humanoid Robot," *Proc. of the 2006 IEEE Int. Conf. on Robotics and Automation*, Orlando, 2006, pp. 1674-1679.

[11] D. Vischer and O. Khatib, "Design and Development of High-performance Torque Controlled Joints," *IEEE Trans. on Robotic and Automation*, vol. 11, no. 4, August 1995, pp. 537-544.

[12] "*Multi-axis F/T Sensor*," ATI Industrial Automation, [Online], Available: http://www.ati-ia.com

0-7695-2738-8/07 $20.00 © 2007 IEEE